Nonreciprocity as a generic route to traveling states

Zhihong You[a,1], Aparna Baskaran[b], and M. Cristina Marchetti[a,1]

[a]Department of Physics, University of California, Santa Barbara, CA 93106; and [b]Martin Fisher School of Physics, Brandeis University, Waltham, MA 02453

Contributed by M. Cristina Marchetti, June 24, 2020 (sent for review May 22, 2020; reviewed by Sharon C. Glotzer and David R. Nelson)

We examine a nonreciprocally coupled dynamical model of a mixture of two diffusing species. We demonstrate that nonreciprocity, which is encoded in the model via antagonistic cross-diffusivities, provides a generic mechanism for the emergence of traveling patterns in purely diffusive systems with conservative dynamics. In the absence of nonreciprocity, the binary fluid mixture undergoes a phase transition from a homogeneous mixed state to a demixed state with spatially separated regions rich in one of the two components. Above a critical value of the parameter tuning nonreciprocity, the static demixed pattern acquires a finite velocity, resulting in a state that breaks both spatial and time-reversal symmetry, as well as the reflection parity of the static pattern. We elucidate the generic nature of the transition to traveling patterns using a minimal model that can be studied analytically. Our work has direct relevance to nonequilibrium assembly in mixtures of chemically interacting colloids that are known to exhibit nonreciprocal effective interactions, as well as to mixtures of active and passive agents where traveling states of the type predicted here have been observed in simulations. It also provides insight on transitions to traveling and oscillatory states seen in a broad range of nonreciprocal systems with nonconservative dynamics, from reaction–diffusion and prey–predators models to multispecies mixtures of microorganisms with antagonistic interactions.

traveling patterns | nonreciprocity | PT symmetry breaking

Traveling patterns occur ubiquitously in nature. Examples range from oscillating chemical reactions (1–3), to waves of metabolic synchronization in yeast (4), to the spatial spread of epidemics (5–8). Most mathematical models that capture such spatiotemporal dynamics, including reaction–diffusion equations (1, 9–12), excitable systems (13, 14), collections of coupled oscillators (15, 16), and prey–predator equations (17–19), are unified by the fact that the dynamical variables are nonconserved fields (20). In this case, the coupling to birth–death or to other reaction processes provides a promoter–inhibitor mechanism that sets up oscillatory states. In this paper, we demonstrate that traveling patterns can arise in multicomponent systems described by purely diffusive conserved fields from nonreciprocal interactions between species. The appearance of traveling or sustained oscillatory states in a purely diffusive system with no apparent external forcing is unexpected and defies intuition. Our work suggests that nonreciprocity provides a generic mechanism for the establishment of traveling states in the dynamics of conserved scalar fields.

The third law of Newtonian mechanics establishes that interactions are reciprocal: For every action, there is an equal and opposite reaction. While, of course, this remains true at the microscopic level, nonreciprocal effective interactions can occur ubiquitously on mesoscopic scales when interactions are mediated by a nonequilibrium environment (21–25). A striking physical example is realized in diffusiophoretic colloidal mixtures (26–28). Nonreciprocal interactions are also the norm in the living world. Examples are promoter–inhibitor interactions among different cell types (29) and the antagonistic interactions among species in bacterial suspensions (30–34). Social forces that control the behavior of human crowds (35–37) and collective animal behavior (38, 39) are other important examples as well.

To highlight the role of nonreciprocal couplings in driving time-dependent phases, we examine a minimal model of the dynamics of two interdiffusing species, each described by a scalar field ϕ_μ, for $\mu = A, B$. The evolution of each concentration field is governed by a ϕ^4 field theory that allows for a spinodal instability according to model B dynamics (40). When decoupled, each phase field can undergo a Hopf bifurcation describing the transition from a homogeneous state to a phase-separated state composed of dilute and dense phases. The two fields are coupled via cross-diffusion terms with diffusivities $\kappa_{\mu\nu}$. When these couplings are reciprocal, the interaction between the two fields leads to a transition between a mixed state where both fields are homogeneous to a demixed state with distinct regions of high A and low B. Nonreciprocity is introduced by allowing the two cross-diffusivities to have opposite signs and is quantified by $\delta = (\kappa_{BA} - \kappa_{AB})/2$. Nonreciprocal cross-diffusivities drive a second transition through a drift bifurcation to a time-dependent state that breaks parity, where the domains of the demixed regions travel at a constant drift velocity. This transition is closely related to ones previously reported in specific models of prey–predator and reaction–diffusion dynamics (8–11, 17, 18, 41), but occurs here from the coupling of two conserved fields. We demonstrate that the transition to traveling states is a parity and time-reversal (PT) symmetry breaking bifurcation that arises generically from nonreciprocal couplings. The phase diagram obtained from numerical solutions of a one-dimensional (1D) realization of this minimal model in the simplest case where only field A is supercritical, while B is subcritical, that is, the ground state value of field B is simply $\phi_B^g = 0$, is shown in Fig. 1*A*. Tuning the control parameter that drives phase separation of species A (χ_A) and the measure of nonreciprocity δ, we observe three distinct states: a mixed state where both fields are homogeneous, a static demixed state

Significance

Effective interactions that break action–reaction symmetry are ubiquitous in systems where interactions are mediated by a nonequilibrium environment. They are also the norm in the living world. By examining the dynamics of a diffusing binary mixture, we demonstrate that antagonistic cross-diffusivities can drive the transition from static to traveling spatial patterns. In the context of an analytically tractable model, we elucidate the nature of the transition and demonstrate that the emergence of traveling or oscillating patterns is a generic consequence of nonreciprocity in multispecies systems described by scalar fields. Our work is directly relevant to the understanding and control of nonequilibrium assembly in mixtures of chemically interacting colloids.

Author contributions: Z.Y., A.B., and M.C.M. designed research, performed research, and wrote the paper.

Reviewers: S.C.G., University of Michigan–Ann Arbor; and D.R.N., Harvard University.

The authors declare no competing interest.

Published under the PNAS license.

[1]To whom correspondence may be addressed. Email: youz@ucsb.edu or cmarchetti@ucsb.edu.

This article contains supporting information online at https://www.pnas.org/lookup/suppl/doi:10.1073/pnas.2010318117/-/DCSupplemental.

First published August 4, 2020.

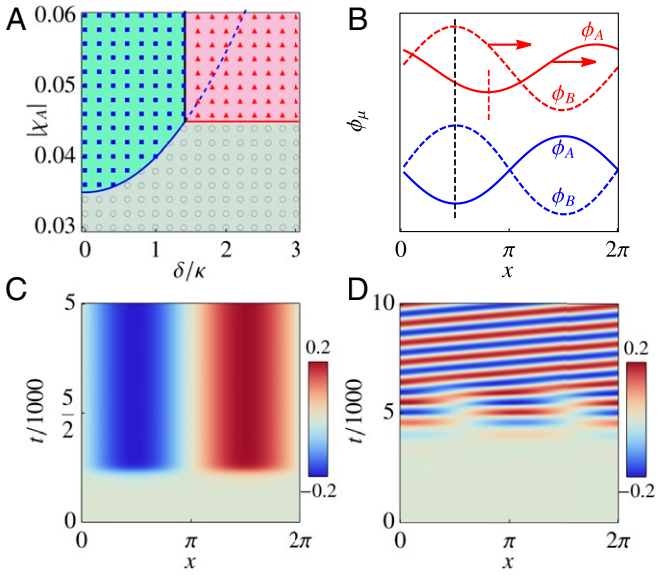

Fig. 1. (*A*) State diagram spanned by δ/κ and χ_A. The system has three distinct states: homogeneous (gray, circles), static patterns or demixed (cyan, rectangles), and traveling patterns (pink, triangles). Symbols indicate results from the simulations, while the lines marking the boundaries of the colored domains are obtained from the stability analysis of the one-mode model. The static demixed state exists in the region between the black and the dashed blue lines, but is unstable. (*B*) Examples of spatial variations of $\phi_A(x)$ (solid lines) and $\phi_B(x)$ (dashed lines) in the static (blue) and traveling (red) states. (*C* and *D*) Spatiotemporal patterns of $\phi_A(x, t)$ in the (*C*) static and (*D*) traveling states. In *B*–*D*, we use $\chi_A = -0.05$ and (*C*) $\delta = \kappa$ and (*D*) $\delta = 2\kappa$.

that breaks translational symmetry with out-of-phase spatial modulations of the two fields, and a time-dependent state that additionally breaks reflection and time-reversal symmetry, where the spatial modulation of the demixed state travels at constant velocity. The solid lines are obtained from a one-mode approximation to the continuum model that can be solved analytically and provides an excellent fit to the numerics. Within this one-mode approximation, the transition from the stationary to the traveling state can be understood as an instability of the relative phase of the first Fourier harmonic of the fields. The instability arises because nonreciprocity allows perturbations in the two fields to travel in the same direction, promoting a "run-and-catch" scenario that stabilizes the traveling pattern. While the spatial pattern in the static demixed phase is even in the relative displacement of the two phase fields, nonreciprocity breaks this reflection symmetry in the traveling state, mediating a PT-symmetry-breaking transition. Note that the transition to a PT-broken phase occurs at a finite value of δ, and hence requires sufficiently strong nonreciprocity. Finally, the phase boundary separating the static and traveling patterns in Fig. 1*A* corresponds to a so-called "exceptional point" where the eigenmodes of the matrix controlling the dynamical stability of the system coalesce (42–44). In parallel to our investigation, Saha et al. (45) have also reported traveling density waves in scalar fields with Cahn–Hilliard dynamics and nonreciprocal couplings. The simulations carried out by these authors support our finding that nonreciprocal couplings provide a generic mechanism for breaking time-reversal symmetry and setting spatial patterns in motion.

A microscopic model that displays the phenomenology captured by Fig. 1*A* is a mixture of active and passive Brownian particles, where the active component exhibits motility-induced phase separation, and fluctuations in the density of passive particles can enhance fluctuations in the density of the active fraction via an effective negative cross-diffusivity (46–48). The connection between the active–passive mixture and the dynamics embodied by our model is unfolded in *SI Appendix*. Another realization of this macrodynamics is a binary suspension of colloidal particles where species A attracts species B, but species B repels species A. Such competing interactions have been studied in simple models (49, 50) and can be realized in mixtures of self-catalytic active colloids, where the local chemistry mediates nonreciprocal interactions among the two species, as demonstrated, for instance, in refs. 27 and 28 via numerical simulations.

Continuum Model

We consider a binary mixture described by two conserved phase fields ϕ_A and ϕ_B with Cahn–Hilliard dynamics (51–53) augmented by cross-diffusion,

$$\partial_t \phi_\mu = \boldsymbol{\nabla} \cdot \left[\left(\chi_\mu + \phi_\mu^2 - \gamma_\mu \nabla^2 \right) \boldsymbol{\nabla} \phi_\mu + \kappa_{\mu\nu} \boldsymbol{\nabla} \phi_\nu \right], \qquad [1]$$

where $\mu, \nu = A, B$ and no summation is intended.* In the absence of cross-diffusive couplings ($\kappa_{\mu\nu} = 0$), the fields are decoupled, with ground states $\phi_\mu^g = 0$ for $\chi_\mu > 0$, describing homogeneous states, and $\phi_\mu^g = \pm\sqrt{-3\chi_\mu}$ when $\chi_\mu < 0$, corresponding to phase-separated states.

The cross-diffusivities control interspecies interaction, allowing phase gradient of one species to drive currents of the other species. Equal cross-diffusivities, $\kappa_{AB} = \kappa_{BA} = \kappa$, yield an effective repulsion between the two fields. When sufficiently strong to overcome the entropy of mixing, such a repulsion results in the formation of spatial domains of high/low ϕ_A/ϕ_B, that is, a demixed state. Here, in contrast, we introduce nonreciprocity by allowing these two quantities to have opposite signs, as can, for instance, be achieved in mixtures of active and passive Brownian particles (*SI Appendix*, section VI) or in mixtures of colloids with competing repulsive and attractive interactions (*SI Appendix*, section VI).† We tune the degree of nonreciprocity $\delta > 0$ by letting

$$\begin{aligned} \kappa_{AB} &= \kappa - \delta, \\ \kappa_{BA} &= \kappa + \delta. \end{aligned} \qquad [2]$$

As shown below, this nonreciprocity breaks PT symmetry and gives rise to spatiotemporal patterns of ϕ_A and ϕ_B that break both spatial and temporal translational symmetry.

We have studied, numerically, Eq. **1** in a 1D box of length $L = 2\pi$, for the case where $\chi_A < 0$ and $\chi_B > 0$, and ignoring ϕ_B^2 in the self-diffusivity. The results are easily generalized to the case where both components are supercritical ($\chi_A < 0$ and $\chi_B < 0$) and to higher dimensions (*SI Appendix*, sections IV and V), but remain qualitatively unchanged. We have integrated Eq. **1** with a fourth-order central difference on a uniform grid with spacing $h = 2\pi/64$. To march in time, we use a second-order, 128-stage Runge–Kutta–Chebyshev scheme with a time step $\Delta t = 0.1$ (56, 57). All simulations start from nearly uniform phase fields, where weak random fluctuations are added on top of the initial compositions $\phi_A^0 = 0$ and $\phi_B^0 = 0$. We fix the values of the parameters as $\gamma_A = 0.04$, $\gamma_B = 0$, $\chi_B = 0.005$, and $\kappa = 0.005$, and study how the system dynamics changes with χ_A and δ.

We find three distinct states by varying χ_A and δ, as summarized in Fig. 1*A*. When the cross-diffusivities are reciprocal

*The natural coupling of two scalar fields with model B dynamics coming from a term $\sim g\phi_A^2\phi_B^2$ in the free energy density is known to yield a rich phase diagram with the possibility of tetracritical points and first-order transitions (54, 55), as pointed out to us by David Nelson. We plan to explore the effect of nonreciprocal biquadratic couplings of this type in future work.

†We note that, in a binary mixture of diffusing particles, the cross-diffusivities would differ, as each $\kappa_{\mu\nu}$ would depend on the concentration of the two species as required to maintain detailed balance, but they would always have the same sign.

($\delta = 0$), by increasing $|\chi_A|$, the system undergoes a Hopf bifurcation from a homogeneous state (gray circles) to a demixed state (blue rectangles) where the two fields are spatially modulated with alternating regions of high ϕ_A/low ϕ_B (Fig. 1 *B* and *C*). This state is stabilized by the cubic term in Eq. **1**, as in conventional Cahn–Hilliard models. Above a critical value of δ, the demixed state undergoes a second bifurcation to a state where the domains of high ϕ_A/low ϕ_B travel at a constant speed (red triangles in Fig. 1 *A*, see also Fig. 1 *B* and *D* for spatiotemporal patterns). The velocity of the traveling pattern provides an order parameter for this transition, and the direction of motion is picked spontaneously. The opposite signs of the cross-diffusivities provide effective antagonistic repulsive and attractive interactions between the two fields. The drift bifurcation is triggered by the nucleation of a phase shift in the spatial modulation of the two fields that allows species A to outrun B, while B tries to catch up with A. At weak nonreciprocity, species A is too slow to escape from B, and the static pattern is restored. Strong nonreciprocity, on other hand, allows species A to outrun B. As the distance between the two increases, A gradually slows down while B speeds up until the two share a common speed and become trapped in a steady traveling state. This "run-and-catch" scenario is quantified below with a simple one-mode analysis of our dynamical equations that captures the behavior quantitatively. The transitions between the various states obtained from the one-mode approximation are shown as solid lines in Fig. 1*A* and provide an excellent fit to the numerics in one dimension. Finally, as discussed further below, the transition is associated with the breaking of reflection symmetry or parity of the spatial modulations, as well as of time-reversal symmetry, and hence provides a realization of a PT-breaking transition.

We show, in *SI Appendix*, that the same scenario applies qualitatively in two dimensions. In this case, in addition to traveling spatial structures, we also observe oscillatory patterns that are absent in one dimension. In the oscillatory state, the system organizes into high/low concentration region of each species that periodically split and merge. The frequency of oscillation increases with δ, suggesting that the oscillating states are a richer manifestation of nonreciprocity and of the "run-and-catch" mechanism that controls the dynamics in one dimension. Both traveling and oscillatory states appear to be stable and coexist at high δ, with the state selection being controlled by initial conditions. This suggests that it would be interesting to go beyond the deterministic model considered here to examine the role of noise. A full study of 2D systems will be reported elsewhere.

One-Mode Approximation

To uncover the physics behind the PT-breaking bifurcation, we expand the fields ϕ_μ in a Fourier series as $\phi_\mu(x,t) = \sum_{j=-\infty}^{\infty} \hat{\phi}_\mu^j(t) e^{iq_j x}$, where $\hat{\phi}_\mu^j = (2\pi)^{-1}\int_0^{2\pi} dx \phi_\mu e^{-iq_j x}$ is the amplitude of mode j. Substituting this in Eq. **1**, and applying the Galerkin method (58), one obtains a set of coupled ordinary differential equations for the Fourier amplitudes. For the 1D model described above, we have verified numerically that only the first Fourier mode $q_1 = 1$ is activated. We can then replace the original partial differential equations with a single-mode approximation, given by

$$\frac{d\hat{\phi}_A^1}{dt} = -\left(\alpha_A + |\hat{\phi}_A^1|^2\right)\hat{\phi}_A^1 - (\kappa - \delta)\hat{\phi}_B^1, \qquad \textbf{[3a]}$$

$$\frac{d\hat{\phi}_B^1}{dt} = -\alpha_B\hat{\phi}_B^1 - (\kappa + \delta)\hat{\phi}_A^1, \qquad \textbf{[3b]}$$

where $\alpha_A = \chi_A + \gamma_A + (\phi_A^0)^2$ can be negative and $\alpha_B = \chi_B > 0$. When $\chi_B > 0$, the cubic term in the dynamics of ϕ_B simply provides a higher-order damping and can be neglected. Writing the complex amplitudes in terms of amplitudes and phases as $\hat{\phi}_\mu^1 = \rho_\mu e^{i\theta_\mu}$, Eq. **3** can be written as

$$\dot{\rho}_A = -(\alpha_A + \rho_A^2)\rho_A - (\kappa - \delta)\rho_B\cos\theta, \qquad \textbf{[4a]}$$

$$\dot{\rho}_B = -\alpha_B\rho_B - (\kappa + \delta)\rho_A\cos\theta, \qquad \textbf{[4b]}$$

$$\dot{\theta} = [(\kappa - \delta)\rho_B/\rho_A + (\kappa + \delta)\rho_A/\rho_B]\sin\theta, \qquad \textbf{[4c]}$$

$$\dot{\Phi} = [(\kappa - \delta)\rho_B/\rho_A - (\kappa + \delta)\rho_A/\rho_B]\sin\theta, \qquad \textbf{[4d]}$$

where $\theta \equiv \theta_A - \theta_B$ and $\Phi \equiv \theta_A + \theta_B$ are the difference and sum of the two phases. Note that the sum phase Φ is slaved to the other quantities. A broken PT pattern traveling at constant velocity corresponds to $\dot{\rho}_A = \dot{\rho}_B = \dot{\theta} = 0$ and $\dot{\Phi} = \text{constant}$, which requires $\sin\theta \neq 0$ and $(\kappa - \delta)\rho_B/\rho_A + (\kappa + \delta)\rho_A/\rho_B = 0$, or, equivalently, $\kappa_{AB}\rho_B^2 = -\kappa_{BA}\rho_A^2$; hence the two cross-diffusivities must have opposite signs. As we will see below, this is a necessary but not sufficient condition for the existence of the traveling state. Next, we examine the fixed points of Eqs. **4a–4c** and their stability.

Fixed Points. There are three fixed points: a trivial fixed point (F_H) with $\rho_A = \rho_B = 0$ (θ and Φ are undetermined), corresponding to a homogeneous mixed state, and two nontrivial fixed points, corresponding to static (F_S) and traveling (F_T) demixed states. The state F_S describes out-of-phase spatial variations of the two phases, with $\theta^s = \pi$ and

$$\rho_A^s = \left(\frac{\kappa^2 - \delta^2 - \alpha_A\alpha_B}{\alpha_B}\right)^{1/2}, \qquad \textbf{[5a]}$$

$$\rho_B^s = (\kappa + \delta)\rho_A^s/\alpha_B, \qquad \textbf{[5b]}$$

while Φ remains undetermined. This solution, of course, only exists provided $\alpha_A\alpha_B < \kappa^2 - \delta^2$. Since $\alpha_B > 0$, the onset of the static demixed state requires $\alpha_A < 0$ to drive the growth of ρ_A, which is then saturated by the cubic damping in Eq. **4a**. Interspecies interactions modulate the pattern, resulting in out-of-phase spatial variations of ϕ_A and ϕ_B, while $\dot{\theta}_A = \dot{\theta}_B$ remains zero, that is, the modulation is static. Note that, in this state, the two fields, although out of phase, have the same parity, either both even or both odd functions of x.

The F_T state is a spatial modulation traveling at constant speed

$$v = \dot{\Phi}^t/2 = \pm\sqrt{\delta^2 - \delta_c^2} \sim (\delta - \delta_c)^{1/2}, \qquad \textbf{[6]}$$

with $\delta_c = \sqrt{\kappa^2 + \alpha_B^2}$ as the critical value of nonreciprocity required for the establishment of the traveling pattern, and

$$\rho_A^t = (-\alpha_A - \alpha_B)^{1/2}, \qquad \textbf{[7a]}$$

$$\rho_B^t = \sqrt{(\delta + \kappa)/(\delta - \kappa)}\ \rho_A^t, \qquad \textbf{[7b]}$$

$$\theta^t = \arccos\left(-\sqrt{\frac{\alpha_B^2}{\delta^2 - \kappa^2}}\right). \qquad \textbf{[7c]}$$

As we will see below, the speed v provides the order parameter for the transition from the static to the traveling state. This latter, of course, only exists when $\kappa - \delta < 0$, or, more specifically, it requires both $\alpha_A < -\alpha_B$ and $\delta^2 \geq \kappa^2 + \alpha_B^2$, that is, strong enough nonreciprocity. It arises because a solution with $\sin\theta \neq 0$ allows each field to travel at a finite velocity $v_\mu = \dot{\theta}_\mu$. The direction of each v_μ is set by fluctuations or initial conditions. As shown in Fig. 2, the velocity of the traveling modulation and the spatial profiles of the two fields obtained from the one-mode approximation provide an excellent fit to those extracted from

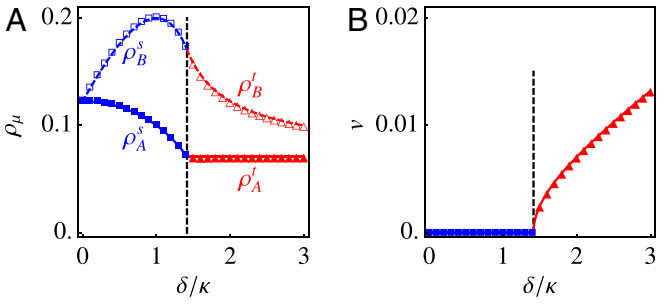

Fig. 2. (*A*) Comparison of the amplitude of the first Fourier modes as obtained from simulations (symbols) and the one-mode approximations (lines): ρ_A (solid line and filled symbols) and ρ_B (dashed line and empty symbols) as functions of δ/κ. (*B*) Velocity of the traveling pattern as a function of δ/κ from simulations (symbols) and one-mode approximation (line). In both *A* and *B*, the black vertical dashed line denotes the critical value $\delta_c/\kappa = (1+\alpha_B^2/\kappa^2)^{1/2}$ of the static-to-traveling transition. $\chi_A = -0.05$ is used in *A* and *B*.

numerical solution of Eq. **1**. As discussed below, the traveling pattern breaks the reflection symmetry (parity) of the static one, as well as time-reversal invariance.

Linear Stability Analysis. A linear stability analysis of the fixed points yields the boundaries between the various states shown in Fig. 1*A* and provides a clear understanding of the mechanism of the drift instability. Linearizing Eq. **3** about the homogeneous state reveals that, in this state, the dynamics of fluctuations is controlled by two eigenvalues given by

$$\lambda_\pm = -\frac{1}{2}(\alpha_A+\alpha_B) \pm \frac{1}{2}\sqrt{(\alpha_A-\alpha_B)^2+4(\kappa^2-\delta^2)}. \qquad [8]$$

If $\delta^2 < \kappa^2 + (\alpha_A-\alpha_B)^2/4$, the eigenvalues are real. The largest eigenvalue λ_+ becomes positive, signaling an instability, when $\delta^2 = \kappa^2 - \alpha_A\alpha_B$. This diffusive instability is displayed as a blue line in Fig. 1*A*. It is a supercritical pitchfork bifurcation, where the trivial steady-state F_H undergoes spontaneous breaking of translational symmetry, leading to the transition to the static phase-separated state F_S. Conversely, when $\delta^2 > \kappa^2 + (\alpha_A - \alpha_B)^2/4$, the eigenvalues are complex conjugate. The state F_H can still become unstable when $\alpha_A < -\alpha_B$, albeit now via an oscillatory instability shown as a red line in Fig. 1*A*.

Further insight is gained by examining the stability of F_S. This requires the analysis of the eigenvalues of the 3×3 matrix obtained by linearizing Eqs. **4a–4c**. Details are given in *SI Appendix*. Note that the matrix is block diagonal, coupling separately the two amplitudes and the phase difference θ. One finds that the instability is driven by the growth of fluctuations in the relative phase θ that become unstable when $\delta > \delta_c$. This boundary $\delta = \delta_c$ corresponds to the appearance of F_T and is shown as a black line in Fig. 1*A*. The instability of the relative phase is associated with the "run-and-catch" scenario described earlier and signals the transition to a state where the two fields have a constants phase lag (different from π), while traveling with a common speed.

To highlight the mechanism responsible for the traveling pattern, note that the velocities of the field modulations $v_\mu = \dot{\theta}_\mu$ are given by $v_A = \kappa_{AB}(\rho_B/\rho_A)\sin\theta$ and $v_B = -\kappa_{BA}(\rho_A/\rho_B)\sin\theta$, and hence are identically zero in the static state F_S where $\theta^s = \pi$. Now consider the effect of a small fluctuation in the relative phase by letting $\theta = \pi + \psi$, as shown in Fig. 3*A*. Evaluating the amplitudes at the steady-state values, the velocities are then given by $v_A^s = -(\kappa_{AB}\kappa_{BA}/\alpha_B)\psi$ and $v_B^s = \alpha_B\psi$ (Fig. 3*B*). If the cross-diffusivities κ_{AB} and κ_{BA} have the same sign, the two species move in opposite directions (black and blue arrows in Fig. 3*A*), exerting reciprocal driving forces on each other, and the perturbation ψ decays. On the other hand, if κ_{AB} and κ_{BA} have opposite signs, the two species travel in the same direction (black and red arrows in Fig. 3*A*) and can play run-and-catch with each other. To establish the precise condition for the onset of the traveling state, it is useful to examine the ratio of the two velocity, which is well defined even in the static demixed state and is given by

$$\frac{v_A}{v_B} = -\frac{\kappa_{AB}\rho_B^2}{\kappa_{BA}\rho_A^2} = -\frac{(\kappa-\delta)\rho_B^2}{(\kappa+\delta)\rho_A^2}. \qquad [9]$$

In the stationary demixed state, where $\rho_B^s/\rho_A^s = (\kappa+\delta)/\alpha_B$, we find $v_A^s/v_B^s = (\delta^2-\kappa^2)/\alpha_B^2$. This quantity is shown in Fig. 3*B*. When $v_A^s/v_B^s < 0$ (blue portion of the curve) a small fluctuation $\psi = \theta - \pi$ of the relative phase yields opposite field velocities (blue arrows), while, when $v_A^s/v_B^s > 0$, the velocities are in the same direction (green portion of the curve and green arrows). Only when $v_A^s/v_B^s > 1$, however, is nonreciprocity strong enough to destabilize the static pattern (red line and arrows in Fig. 3*B*). The onset of the traveling state corresponds to $v_A^s = v_B^s$ or $\delta = \delta_c$, as obtained from the linear stability analysis. The condition $v_A = v_B$ provides a general necessary condition for the onset of traveling patterns of two interacting scalar fields.

The equality of the velocities is not, however, sufficient to stabilize the traveling pattern, as the perturbation ψ will keep increasing if $v_A > v_B$ persists. Nonreciprocal interactions come again to the rescue by facilitating the "redistribution" of

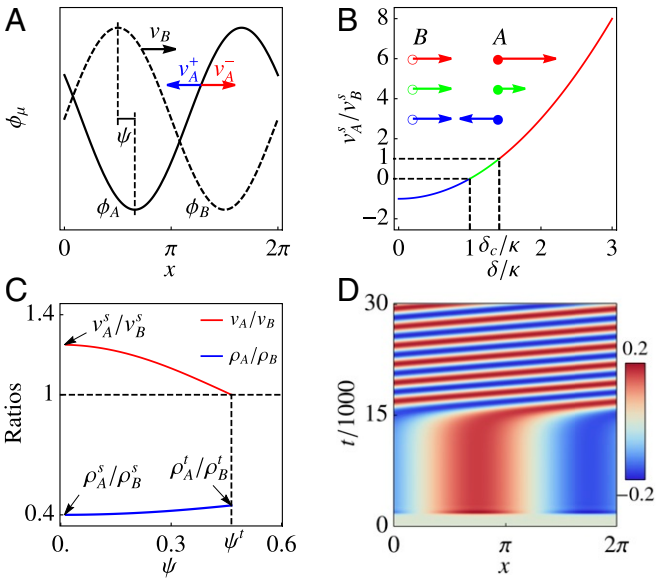

Fig. 3. A pictorial explanation of the "run-and-catch" mechanism that leads to the stable traveling state. (*A*) A phase shift $\psi = \theta - \pi$ of ϕ_A (solid line) and ϕ_B (dashed line) relative to the out-of-phase modulation of the stationary demixed state results in finite velocities for the two fields. For a given v_B (black arrow), v_A is in the opposite (blue) or same (red) direction depending on whether the cross-diffusivities have equal or opposite signs. (*B*) Ratio of velocities of the two species as given by Eq. **9** evaluated at the F_S fixed point as a function of δ/κ. The arrows are a depiction of the velocities obtained for a small finite ψ. Arrow colors correspond to the colors of each portion of the curve. (*C*) Ratio of the velocities (red) and amplitudes (blue) of the two species as functions of $\psi = \theta - \pi$ obtained from a simulation where the static pattern experiences a drift bifurcation and becomes traveling (i.e., *D*). The values at $\psi = 0$ and $\psi = \psi^t = \theta^t - \pi$ agree with those obtained from the one-mode model. The horizontal dashed line corresponds to $v_A/v_B = 1$ and the vertical dashed line is the value ψ^t corresponding to the steady traveling state. (*D*) Spatiotemporal patterns at the onset of the static-to-traveling transition with $\delta/\kappa = 1.5$. $\chi_A = -0.05$ is used.

amplitude growth. Specifically, as ψ increases, both the damping of ρ_A and the activation of ρ_B originating from the nonreciprocal nature of the cross-couplings become weaker (last terms in Eqs. **4a** and **4b**). Consequently, the amplitude ratio ρ_A/ρ_B increases and suppresses the velocity difference until $v_A = v_B$, allowing the development of a steady traveling pattern, as shown in Fig. 3*C*. We have validated this simple picture displayed in Fig. 3*D* by examining numerically the mechanisms of stabilization of the traveling state F_T for δ slightly larger than δ_c.

Static-to-Traveling as a PT-Breaking Transition

The static-to-traveling transition described in this work belongs to a more generic class of PT-breaking transitions (20, 59, 60), which has been studied in optical and quantum systems (60, 61) and, more recently, in polar active fluids with nonreciprocal interactions (44). This type of transition is known to occur at a so-called exceptional point, which is simply a point where the eigenvalues of the matrix that governs the linear stability of a fixed point become equal and its eigenvectors are colinear. While not uncommon in hydrodynamics when fluids are driven by external forces or in systems described by nonconserved fields, the occurrence of such a transitions giving rise to nontrivial traveling structures in conserved systems is unexpected.

The dynamics of our coupled fields can be written in a compact form as

$$\partial_t \begin{pmatrix} \phi_A \\ \phi_B \end{pmatrix} = \mathbf{M} \cdot \begin{pmatrix} \phi_A \\ \phi_B \end{pmatrix}, \qquad [10]$$

where the 2×2 matrix operator $\mathbf{M} = \mathbf{M}[\phi_A^2, \phi_B^2, \nabla^2]$ can be inferred from Eq. **1**. In the static, spatially modulated solution corresponding to the demixed state, the two fields ϕ_A and ϕ_B are out of phase, but have the same parity under spatial inversion, $x \to -x$, as required by the symmetry of $\mathbf{M}$. The domains become traveling by acquiring a component of the opposite parity that breaks the relative parity of the two fields, as described in ref. 20. Hence the transition to the traveling state breaks both parity and time-reversal invariance.

This is most easily understood in the context of the one-mode approximation by considering a static F_S solution of the form $\phi_B = \rho_B \cos(x)$ and $\phi_A = \rho_A \cos(x + \pi)$. Both fields are even and are out of phase, but have different amplitudes. A perturbation ψ in the phase difference yields $\phi_A = \rho_A \cos(x + \pi + \psi) = \rho_A [-\cos\psi \cos x + \sin\psi \sin x]$, breaking parity as ϕ_A now acquires an odd component. The response to such a perturbation is governed by Eq. **4c** linearized about the steady state for $\delta \to \delta_c$, which is given by

$$\dot{\psi} \simeq \frac{2\delta_c(\delta - \delta_c)}{\alpha_B}\psi. \qquad [11]$$

For $\delta < \delta_c$, the odd component of ϕ_A proportional to ψ decays, restoring the parity of the static solution. For $\delta > \delta_c$, ψ grows to a finite value, destabilizing the static state. As a result, ϕ_A acquires a finite odd component, breaking the parity of the static solution. Meanwhile, near the transition, Eq. **4d** gives $\dot{\Phi}_T \simeq 2\alpha_B\psi$, resulting in a finite $\dot{\Phi}$ for $\delta > \delta_c$ and breaking time-reversal symmetry.

Discussion and Outlook

We have shown that nonreciprocal effective interactions in a minimal model of conserved coupled fields with purely diffusive dynamics lead to a PT-breaking transition to traveling spatially modulated states. While the emergence of traveling spatiotemporal patterns is well known in reaction–diffusion, prey–predators, and related models, its appearance in the dynamics of conserved fields without external forcing is surprising. Although the work presented here is limited to a minimal model in one dimension, preliminary results shown in *SI Appendix* indicate that the same mechanism is at play in two dimensions, as well as in mixtures of active and passive particles and of particles interacting via competing repulsive and attractive interactions, as may be realized in phoretic colloidal mixtures. We speculate, therefore, that the mechanism described here through which nonreciprocal effective couplings grant motility to static spatial modulations may be a generic property of multispecies systems describes by scalar fields.

The type of static-to-traveling transition described here occurs in Mullins–Sekerka models of crystal growth (62), Keller–Segel, prey–predator and reaction–diffusion models of population dynamics and general systems described by nonconserved dynamical fields, where it has been referred to as a drift bifurcation (18, 20, 41). It occurs in these systems when a stationary or standing wave pattern generated through a conventional Hopf bifurcation undergoes a second instability to a traveling state. The drift bifurcation can be understood, using amplitude equations, as arising from the antagonistic coupling of at least two leading modes (41). Here we show that a similar mechanism can be at play in multispecies systems with dynamics described by two conserved scalar fields coupled by sufficiently strong nonreciprocal interactions. When sufficiently strong, nonreciprocity leads to an effective antagonistic repulsion/attraction between the two fields, resulting in the run-and-catch mechanism described here that yields a PT-symmetry-breaking transition. Our one-mode approximation provides a minimal analytic description of this generic mechanism, where $v = \dot{\Phi}/2$ serves as the order parameter for the transition.

A scenario similar to the one described here was recently identified in a binary Vicsek model with nonreciprocal interactions (44). The mechanisms promoting the onset of a state with broken PT are the same in both models, but the outcomes are distinct due to the different symmetry of the two systems. In ref. 44, it is suggested that nonreciprocal interaction in a polar system may generically result in macroscopically chiral phases. Here, in contrast, we consider a scalar model with conserved dynamics and demonstrate that, in this case, nonreciprocity generically yields spatially inhomogeneous traveling states through the same type of PT-breaking transition. Together, these works pave the way to the study of the interplay of nonreciprocity and spontaneously broken symmetry, suggesting a path to the classification of a new type of PT-breaking transitions.

Understanding and quantifying the role of nonreciprocity in controlling nonequilibrium pattern formation has direct implications for the assembly of chemically interacting colloids, where different particles naturally produce different chemicals mediating nonreciprocal couplings that can induce the type of chasing behavior seen in our work. It also provides a general framework for understanding the nature of wave and oscillatory behavior seen ubiquitously in systems with nonconserved fields, from diffusion reaction to prey–predator and population dynamics models. Our predictions can be tested in detailed simulations of active–passive colloidal mixtures or of particles with antagonistic interactions, as well as experiments in mixtures of chemically driven microswimmers.

Our work opens up many directions of inquiry. Obvious extensions are to higher dimensions where we expect a richer phase diagram and to systems with birth and death processes that select a scale of spatial patterns (63). The exploration of the role of nonreciprocal interactions in active matter systems with broken orientational symmetry, either polar or nematic, is only beginning (44) and promises to reveal a rich phenomenology. Chemically mediated or other nonequilibrium couplings can often be time delayed, which can provide an additional, possibly competing mechanism for the emergence of oscillatory

behavior. Finally, an important open problem is understanding how nonreciprocity arises as an emergent property in systems with microscopic reciprocal interactions, such as active–passive mixtures.

ACKNOWLEDGMENTS. M.C.M. thanks Mark Bowick and Vincenzo Vitelli for illuminating discussions. M.C.M. and Z.Y. were primarily supported by the NSF through the Materials Science and Engineering Center at University of California, Santa Barbara, Grant DMR-1720256 (iSuperSeed), with additional support from Grants DMR-1609208 and PHY-1748958 at the Kavli Institute for Theoretical Physics (KITP). A.B. was supported, in part, by Grants MRSEC-1420382 and BSF-2014279. Finally, the work greatly benefitted from the intellectual stimulation provided by the virtual KITP programs during lockdown.

1. R. Field, M. Burger, *Oscillations and Traveling Waves in Chemical Systems* (Wiley, 1985).
2. S. Weiss, R. D. Deegan, Weakly and strongly coupled Belousov-Zhabotinsky patterns. *Phys. Rev. E* **95**, 022215 (2017).
3. S. N. Semenov *et al.*, Autocatalytic, bistable, oscillatory networks of biologically relevant organic reactions. *Nature* **537**, 656–660 (2016).
4. J. Schütze, T. Mair, M. J. Hauser, M. Falcke, J. Wolf, Metabolic synchronization by traveling waves in yeast cell layers. *Biophys. J.* **100**, 809–813 (2011).
5. O. Diekmann, Thresholds and travelling waves for the geographical spread of infection. *J. Math. Biol.* **6**, 109–130 (1978).
6. O. Diekmann, Run for your life. a note on the asymptotic speed of propagation of an epidemic. *J. Differ. Equ.* **33**, 58–73 (1979).
7. G. Abramson, Traveling waves of infection in the hantavirus epidemics. *Bull. Math. Biol.* **65**, 519–534 (2003).
8. S. Wang, W. Liu, Z. Guo, W. Wang, Traveling wave solutions in a reaction-diffusion epidemic model. *Abstr. Appl. Anal.* **2013**, 1–13 (2013).
9. T. Erneux, G. Nicolis, Propagating waves in discrete bistable reaction-diffusion systems. *Phys. Nonlinear Phenom.* **67**, 237–244 (1993).
10. K. Krischer, A. Mikhailov, Bifurcation to traveling spots in reaction-diffusion systems. *Phys. Rev. Lett.* **73**, 3165–3168 (1994).
11. S. Kondo, T. Miura, Reaction-diffusion model as a framework for understanding biological pattern formation. *Science* **329**, 1616–1620 (2010).
12. G. Gambino, M. Lombardo, M. Sammartino, Pattern formation driven by cross-diffusion in a 2d domain. *Nonlinear Anal. R. World Appl.* **14**, 1755–1779 (2013).
13. J. P. Keener, Waves in excitable media. *SIAM J. Appl. Math.* **39**, 528–548 (1980).
14. A. Holden, M. Markus, H. Othmer, *Nonlinear Wave Processes in Excitable Media (NATO Science Series B,* Springer, 2013), vol. 244.
15. H. Hong, S. H. Strogatz, Kuramoto model of coupled oscillators with positive and negative coupling parameters: An example of conformist and contrarian oscillators. *Phys. Rev. Lett.* **106**, 054102 (2011).
16. H. Hong, S. H. Strogatz, Mean-field behavior in coupled oscillators with attractive and repulsive interactions. *Phys. Rev. E* **85**, 056210 (2012).
17. M. A. Tsyganov, J. Brindley, A. V. Holden, V. N. Biktashev, Quasisoliton interaction of pursuit-evasion waves in a predator-prey system. *Phys. Rev. Lett.* **91**, 218102 (2003).
18. V. N. Biktashev, M. A. Tsyganov, Spontaneous traveling waves in oscillatory systems with cross diffusion. *Phys. Rev. E* **80**, 056111 (2009).
19. M. Mobilia, I. Georgiev, U. Täuber, Phase transitions and spatio-temporal fluctuations in stochastic lattice Lotka-Volterra models. *J. Stat. Phys.* **128**, 447–483 (2007).
20. P. Coullet, R. E. Goldstein, G. H. Gunaratne, Parity-breaking transitions of modulated patterns in hydrodynamic systems. *Phys. Rev. Lett.* **63**, 1954–1957 (1989).
21. A. V. Ivlev *et al.*, Statistical mechanics where Newton's third law is broken. *Phys. Rev. X* **5**, 011035 (2015).
22. M. Durve, A. Saha, A. Sayeed, Active particle condensation by non-reciprocal and time-delayed interactions. *Eur. Phys. J. E* **41**, 49 (2018).
23. K. Hayashi, S. i. Sasa, The law of action and reaction for the effective force in a non-equilibrium colloidal system. *J. Phys. Condens. Matter* **18**, 2825–2836 (2006).
24. M. Paoluzzi, M. Leoni, M. C. Marchetti, Fractal aggregation of active particles. *Phys. Rev. E* **98**, 052603 (2018).
25. M. Paoluzzi, M. Leoni, M. C. Marchetti, Collective dynamics of logic active particles. arXiv:2002.01235 (4 February 2020).
26. R. Soto, R. Golestanian, Self-assembly of catalytically active colloidal molecules: Tailoring activity through surface chemistry. *Phys. Rev. Lett.* **112**, 068301 (2014).
27. J. Agudo-Canalejo, R. Golestanian, Active phase separation in mixtures of chemically interacting particles. *Phys. Rev. Lett.* **123**, 018101 (2019).
28. S. Saha, S. Ramaswamy, R. Golestanian, Pairing, waltzing and scattering of chemotactic active colloids. *New J. Phys.* **21**, 063006 (2019).
29. E. Theveneau *et al.*, Chase-and-run between adjacent cell populations promotes directional collective migration. *Nat. Cell Biol.* **15**, 763–772 (2013).
30. S. Pigolotti, R. Benzi, Selective advantage of diffusing faster. *Phys. Rev. Lett.* **112**, 188102 (2014).
31. R. A. Long, F. Azam, Antagonistic interactions among marine pelagic bacteria. *Appl. Environ. Microbiol.* **67**, 4975–4983 (2001).
32. L. Xiong *et al.*, Flower-like patterns in multi-species bacterial colonies. *eLife* **9**, e48885 (2020).
33. D. Yanni, P. Márquez-Zacarías, P. J. Yunker, W. C. Ratcliff, Drivers of spatial structure in social microbial communities. *Curr. Biol.* **29**, R545–R550 (2019).
34. A. I. Curatolo *et al.*, Engineering cooperative patterns in multi-species bacterial colonies. bioRxiv:798827 (11 October 2019).
35. D. Helbing, P. Molnár, Social force model for pedestrian dynamics. *Phys. Rev. E* **51**, 4282–4286 (1995).
36. D. Helbing, I. Farkas, T. Vicsek, Simulating dynamical features of escape panic. *Nature* **407**, 487–490 (2000).
37. N. Bain, D. Bartolo, Dynamic response and hydrodynamics of polarized crowds. *Science* **363**, 46–49 (2019).
38. A. Strandburg-Peshkin *et al.*, Visual sensory networks and effective information transfer in animal groups. *Curr. Biol.* **23**, PR709–R711 (2013).
39. T. Vicsek, A. Zafeiris, Collective motion. *Phys. Rep.* **517**, 71–140 (2012).
40. P. C. Hohenberg, B. I. Halperin, Theory of dynamic critical phenomena. *Rev. Mod. Phys.* **49**, 435–479 (1977).
41. S. Fauve, S. Douady, O. Thual, Drift instabilities of cellular patterns. *J. Phys. II* **1**, 311–322 (1991).
42. T. Kato, *Perturbation Theory for Linear Operators, Classics in Mathematics* (Springer, 1966).
43. C. M. Bender, Making sense of non-Hermitian Hamiltonians. *Rep. Prog. Phys.* **70**, 947–1018 (2007).
44. M. Fruchart, R. Hanai, P. B. Littlewood, V. Vitelli, Phase transitions in non-reciprocal active systems. arXiv:2003.13176 (19 May 2020).
45. S. Saha, J. Agudo-Canalejo, R. Golestanian, Scalar active mixtures: The non-reciprocal Cahn-Hilliard model. arXiv:2005.07101 (14 May 2020).
46. A. Wysocki, R. G. Winkler, G. Gompper, Propagating interfaces in mixtures of active and passive Brownian particles. *New J. Phys.* **18**, 123030 (2016).
47. R. Wittkowski, J. Stenhammar, M. E. Cates, Nonequilibrium dynamics of mixtures of active and passive colloidal particles. *New J. Phys.* **19**, 105003 (2017).
48. M. Agrawal, I. R. Bruss, SC. Glotzer, Tunable emergent structures and traveling waves in mixtures of passive and contact-triggered-active particles. *Soft Matter* **13**, 6332–6339 (2017).
49. D. Yllanes, M. Leoni, M. C. Marchetti, How many dissenters does it take to disorder a flock?*New J. Phys.* **19**, 103026 (2017).
50. L. L. Bonilla, C. Trenado, Contrarian compulsions produce exotic time-dependent flocking of active particles. *Phys. Rev. E* **99**, 012612 (2019).
51. J. W. Cahn, J. E. Hilliard, Free energy of a nonuniform system. I. Interfacial free energy. *J. Chem. Phys.* **28**, 258–267 (1958).
52. C. M. Elliott, "The Cahn-Hilliard model for the kinetics of phase separation" in *Mathematical Models for Phase Change Problems* (Birkhäuser, 1989), pp. 35–73.
53. E. Khain, L. M. Sander, Generalized Cahn-Hilliard equation for biological applications. *Phys. Rev. E* **77**, 051129 (2008).
54. K. S. Liu, M. E. Fisher, Quantum lattice gas and the existence of a supersolid. *J. Low Temp. Phys.* **10**, 655–683 (1973).
55. F. Wegner, On the magnetic phase diagram of (Mn, Fe)WO4 wolframite. *Solid State Commun.* **12**, 785–787 (1973).
56. W. Hundsdorfer, J. Verwer, *Numerical Solution of Time-dependent Advection-Diffusion-Reaction Equations* (Springer Series in Computational Mathematics, Springer, 2003), vol. 33.
57. J. G. Verwer, W. H. Hundsdorfer, B. P. Sommeijer, Convergence properties of the Runge-Kutta-Chebyshev method. *Numer. Math.* **57**, 157–178 (1990).
58. J. S. Hesthaven, S. Gottlieb, D. Gottlieb, *Spectral Methods for Time-dependent Problems* (Cambridge Monographs on Applied and Computational Mathematics, Cambridge University Press, 2007), vol. 21.
59. R. El-Ganainy *et al.*, Non-hermitian physics and pt symmetry. *Nat. Phys.* **14**, 11–19 (2018).
60. R. Hanai, P. B. Littlewood, Critical fluctuations at a many-body exceptional point. arXiv:1908.03243 (8 August 2019).
61. Z. Lin *et al.*, Unidirectional invisibility induced byPT-symmetric periodic structures. *Phys. Rev. Lett.* **106**, 213901 (2011).
62. W. W. Mullins, R. F. Sekerka, Stability of a planar interface during solidification of a dilute binary alloy. *J. Appl. Phys.* **35**, 444–451 (1964).
63. M. E. Cates, D. Marenduzzo, I. Pagonabarraga, J. Tailleur, Arrested phase separation in reproducing bacteria creates a generic route to pattern formation. *Proc. Natl. Acad. Sci. U.S.A.* **107**, 11715–11720 (2010).